Influence of magnetocaloric and electrocaloric effects on spin conductivity of an open Fermi-Hubbard lattice

Vladimir P. Villegas [1]

10 November 2023

[1]Department of Mathematics and Physics,
College of Science, University of Santo Tomas,
España Blvd., Sampaloc 1008 Manila

Table of Contents

Magnetocaloric and electrocaloric effects

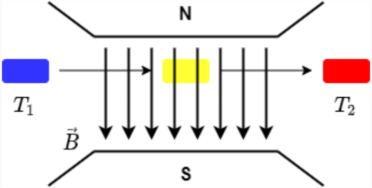

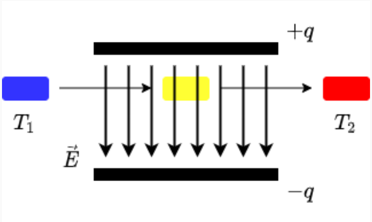

Figure 1: Schematic diagrams of (left) magnetocaloric and (right) electrocaloric effects.

Open Fermi-Hubbard model

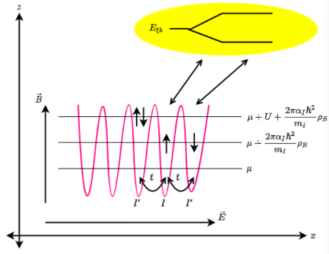

Figure 2: Schematic diagram of the open Fermi-Hubbard (FH) model with external EM fields [1].

- Dilute gas trapped by superposed lasers [2]
- Nearest-neighbor tunneling (t), two-particle interaction (U), chemical potential (μ)
- Applications: spin-$\frac{1}{2}$ cuprates [3, 4]

External EM field effects on entropy

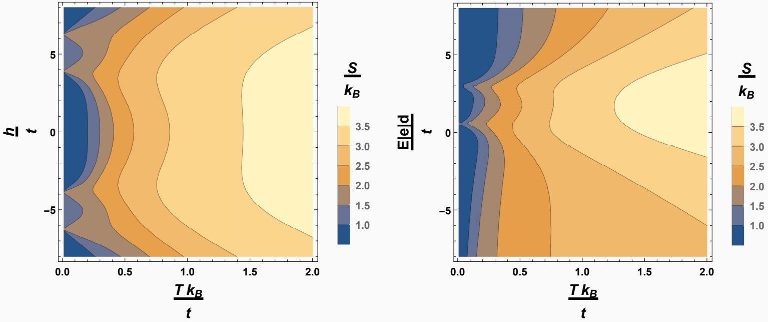

Figure 3: Density plots of entropy S when (left) electric scalar potential $E|e|d = 0$ while magnetic vector potential h is varied and (right) $h = 3t$ while $E|e|d$ is varied [1, 5].

External EM field effects on heat capacity

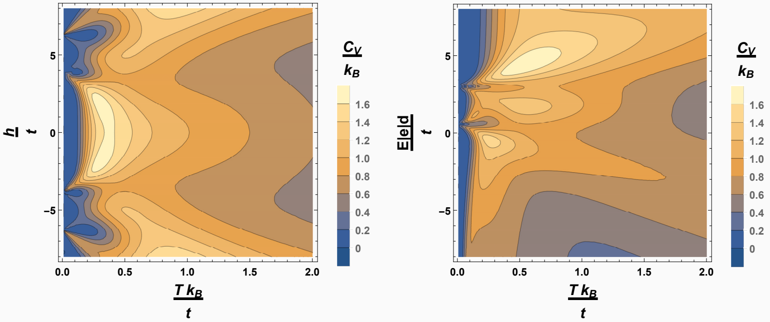

Figure 4: Density plots of heat capacity at constant volume C_V when (left) electric scalar potential $E|e|d = 0$ while magnetic vector potential h is varied and (right) $h = 3t$ while $E|e|d$ is varied [1, 5].

Quantum heat engines

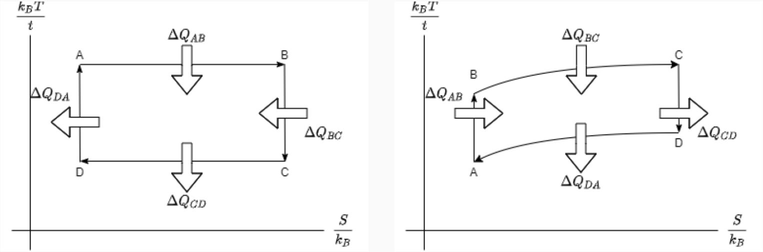

Figure 5: Schematic diagrams of quantum (left) Carnot and (right) Otto heat engines [6].

- Processes achieved by adjusting external fields
- Reverse cycle: quantum refrigerator

Spin transport

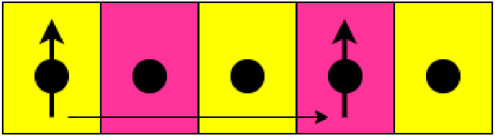

Figure 6: Schematic diagram [7]

- Charge not necessarily transported simultaneously [8]
- High T: spin and charge transport indistinguishable

Table of Contents

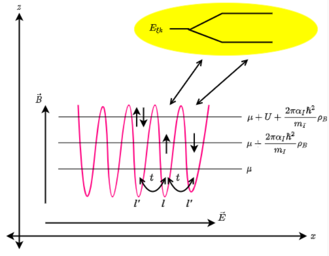

Total Hamiltonian [9, 10]

$$\hat{H} = \hat{H}_S + \hat{H}_B + \hat{H}_{\text{int}} \tag{1}$$

Lattice Hamiltonian

Elastic Fermi-Hubbard model [11, 12, 13]:

$$\begin{aligned}\hat{H}_S =& - t \sum_{s_s,\kappa_s} \left[-2t\cos\left(\kappa_s \delta_s - \mu - \frac{h}{2} s_s \right) \right] \hat{n} s_s \kappa_s \\ & - E|e|\delta_s \sum_{s_s,\kappa_s,\kappa_s'} \left(\hat{n}_{s_s\kappa_s} - \hat{n}_{s_s\kappa_s'} \right) + \frac{U_0}{N_s} \sum_{\kappa_s,\kappa_s',q_s} \hat{c}^\dagger_{\uparrow\kappa_s - q_s} \hat{c}^\dagger_{\downarrow\kappa_s'+q_s} \hat{c}_{\downarrow\kappa_s'} \hat{c}_{\uparrow\kappa_s} \\ & + \frac{U_e}{N_s} \sum_{s_s,\kappa_s,\kappa_s',q_s} \hat{c}^\dagger_{s_s\kappa_s - q_s} \hat{c}^\dagger_{s_s\kappa_s'+q_s} \hat{c}_{s_s\kappa_s'} \hat{c}_{s_s\kappa_s}\end{aligned} \tag{2}$$

Open quantum system

Bath Hamiltonian [10]: Mean-field approximation

$$\hat{H}_B = \sum_{s_B} \mathcal{E}_{\kappa_B} \hat{n}_{s_B \kappa_B} \tag{3}$$

Interaction between optical lattice and gas bath:

$$\hat{H}_{\text{int}} = \frac{2\pi\alpha_I \hbar^2}{m_I} \sum_{s_s, l} \hat{n}_{s_s l} \left(\rho_B + \frac{1}{V_B} \sum_{s_B} (u^2_{s_B \kappa_B} - v^2_{s_B \kappa_B} + 1) \hat{n}_{s_B \kappa_B} \right) \tag{4}$$

Table of Contents

Statistical mechanical properties

Grand canonical partition function [14]:

$$Z = \mathrm{Tr}\left[e^{-\frac{\hat{H}_{\mathrm{total}}}{k_B T}}\right] \tag{5}$$

Average of any variable A:

$$\langle \hat{A} \rangle = \mathrm{Tr}\left[\hat{A} e^{-\frac{\hat{H}_{\mathrm{total}}}{k_B T}}\right] \tag{6}$$

Consider the thermal fluctuation of $A(T)$.

Coherent state path integral

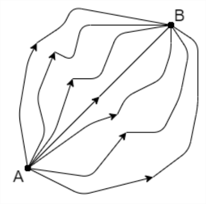

Figure 7: Sum over all possible paths

Temperature as imaginary time:

$$\tau = it \tag{7}$$

Partition function:

$$Z = \int Dc\ Dc^{\dagger} Db\ Db^{\dagger} \exp\left[-\frac{1}{\hbar}\int_0^{\hbar\beta} H_{\text{total}}\left(c(\tau), c^{\dagger}(\tau), b(\tau), b^{\dagger}(\tau)\right)\right] \tag{8}$$

Quantum perspective of current

Ohm's Law:

$$\vec{j}(q,\omega) = \sigma(q,\omega)\vec{E}(q,\omega) \tag{9}$$

Current density operator in quantum mechanics [15]:

$$\vec{j}(q,\omega) = \underbrace{\vec{j}_{\mathrm{P}}(q,\omega)}_{\text{paramgnetic}} + \underbrace{\vec{j}_{\mathrm{D}}(q,\omega)}_{\text{diamagnetic}} \tag{10}$$

Second-quantized current

Charge current [8]:

$$j_{cx}(q,\tau) = it \sum_{s_s,\langle l,l'\rangle} \delta_x \hat{c}^{\dagger}_{s_s l+\delta}(\tau)\, \hat{c}_{s_s l}(\tau)\, e^{iq\left(R_{lx}+\frac{d_x}{2}\right)} \tag{11}$$

Spin current:

$$j_{sx}(q,\tau) = \frac{it}{2} \sum_{s_s,\langle l,l'\rangle} s_s \delta_x \hat{c}^{\dagger}_{s_s l+\delta}(\tau)\, \hat{c}_{s_s l}(\tau)\, e^{iq\left(R_{lx}+\frac{d_x}{2}\right)} \tag{12}$$

Second-quantized conductivity

Kubo formula [15, 16]

$$\sigma_{\eta\nu}(q,\omega) = \frac{i}{\omega}\left[\frac{n_0 e^2}{m}\delta_{\eta\nu} + \Pi_{\eta\nu}(q,\omega)\right] \tag{13}$$

Current-current correlation

$$\Pi_{\eta\nu}\left(q,\omega\right) = \lim_{i\omega_n \to \omega + i\epsilon} \int_0^{\hbar\beta} d\tau \; e^{i\omega\tau} \left\langle T_\tau j_\eta^\dagger\left(q,\tau\right) j_\nu\left(q,0\right)\right\rangle \tag{14}$$

Real part of conductivity

$$\mathrm{Re}\;\sigma_{\eta\nu} = \lim_{q,\omega\to 0} \frac{1}{\omega}\Pi_{\eta\nu}(q,\omega) \tag{15}$$

Table of Contents

Limitations of the study

- One-dimensional
- Half-filling

$$U_0 = \frac{\mu}{2} \tag{16}$$

- Elastic two-particle interaction

$$U_0 = U_e \tag{17}$$

- Bath-induced two-particle interaction

$$\frac{2\pi\alpha_I}{mV_B}\left(u^2_{s_B\kappa_B} - v^2_{s_B\kappa_B} + 1\right) = \frac{1}{4}\mathrm{sgn}\left(U_0\right) \tag{18}$$

Effect of two-particle interactions

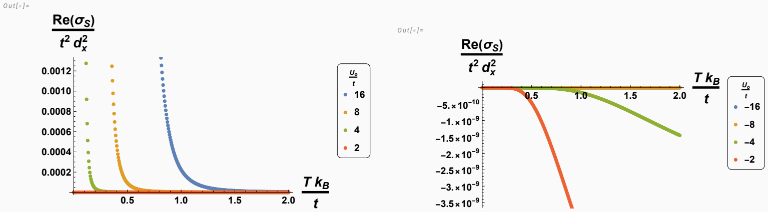

Figure 8: Density plots of spin conductivity σ_S for (left) $U > 0$ and (right) $U < 0$ while $h = E|e|d = 0$.

Attractive regime: Effect of magnetic field

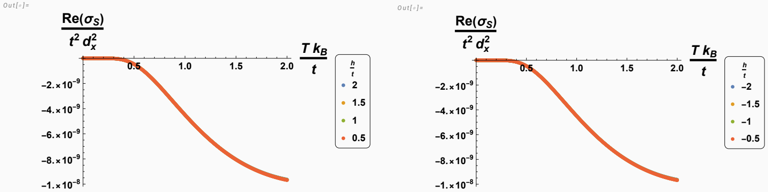

Figure 9: Density plots of spin conductivity σ_S for different values of (left) $h > 0$ and (right) $h < 0$ while $E|e|\delta_x = 0$ and $U = -2t$.

Attractive regime: Effect of electric field

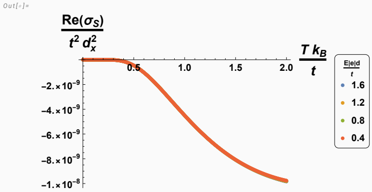

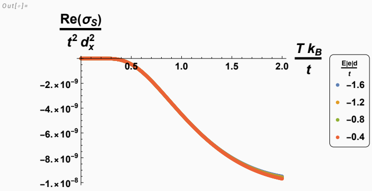

Figure 10: Density plots of spin conductivity σ_S for arbitrary h, different values of (left) $E|e|\delta_x > 0$ and (right) $E|e|\delta_x < 0$ while $U = -2t$.

Repulsive interaction: Effect of magnetic field

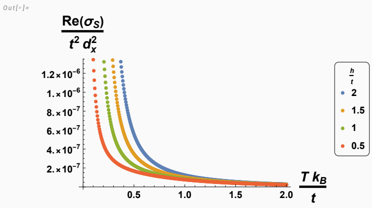

Figure 11: Density plots of spin conductivity σ_S for $E|e|d = 0$, different values of (left) $h > 0$ and (right) $h < 0$ while $U = 2t$.

Repulsive interaction: Effect of electric field

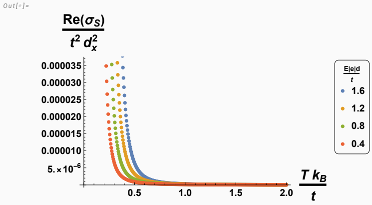

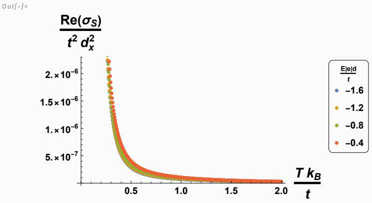

Figure 12: Density plots of spin conductivity σ_S for $h = 2t$, different values of (left) $E|e|\delta_x > 0$ and (right) $E|e|\delta_x < 0$ while $U = 2t$.

Table of Contents

Summary

$U > 0$: increase of conductivity approaching zero temperature

- Finite h increases σ_S at any T
- $E|e|\delta_x > 0$ increases σ_S at any T

$U < 0$: backflow of fermions, uniformity under finite filed

Future direction

- Charge conductivity
- Next-nearest neighbor interaction
- More bath levels
- Hubbard-Heisenberg transition
- Quantum Hall effect
- Seebeck effect

References i

[1] V. P. Villegas and C. D. Villagonzalo.
Refrigeration using magnetocaloric and electrocaloric effects in a Fermi–Hubbard optical dimer exposed to a heat bath.
Physica A, 600:127540, 2022.

[2] T. Esslinger.
Fermi-Hubbard Physics with Atoms in an Optical Lattice.
Annu. Rev. Cond. Matt. Phys., 1(1):129–152, 2010.

[3] T. Balcerzak and K. Szałowski.
Hubbard pair cluster in the external fields. Studies of the polarization and susceptibility.
Physica A, 512:1069–1084, 2018.

References ii

[4] K. Szałowski and T. Balcerzak.
Magnetocaloric and electrocaloric properties of the Hubbard pair cluster.
Journ. Magn. Magn. Mater., 527:167767, 2021.

[5] V. P. Villegas and C. D. Villagonzalo.
Corrigendum and addendum to "Refrigeration using magnetocaloric and electrocaloric effects in a Fermi–Hubbard optical dimer exposed to a heat bath" [Physica A 600 (2022) 127540].
Physica A, 620:128743, 2023.

[6] V. P. Villegas and C. D. Villagonzalo.
Magnetocaloric and electrocaloric heat engine and refrigeration cycles in the open Fermi-Hubbard optical dimer with attractive interactions.
Phys. Lett. A, 481:129011, 2023.

[7] V. P. Villegas and C. D. Villagonzalo.
Caloric effects in an open Fermi–Hubbard optical dimer due to onsite and heat bath-induced two-particle interactions.
J. Magn. Magn. Mater., 564:170094, 2022.

[8] M. Ulaga, J. Mravlje, and J. Kokalj.
Spin diffusion and spin conductivity in the two-dimensional Hubbard model.
Phys. Rev. B, 103:155123, 2021.

[9] H. P. Breuer and F. Petruccione.
The Theory of Open Quantum Systems.
Oxford University Press, 2002.

[10] R. C. F. Caballar, S. Diehl, H. Mäkelä, M. Oberthaler, and G. Watanabe.
Dissipative preparation of phase- and number-squeezed states with ultracold atoms.
Phys. Rev. A, 89:013620, Jan 2014.

[11] D. Jaksch and P. Zoller.
The cold atom Hubbard toolbox.
Ann. Phys., 315(1):52–79, 2005.
Special Issue.

[12] T. Balcerzak and K. Szałowski.
Hubbard pair cluster with elastic interactions. Studies of thermal expansion, magnetostriction and electrostriction.
Physica A, 531:121740, 2019.

[13] T. Balcerzak and K. Szałowski.
Hubbard pair cluster in the external fields. Studies of the chemical potential.
Physica A, 468:252–266, 2017.

[14] L E Reichl.
A Modern Course in Statistical Physics.
Wiley-VCH, Weinheim, Fourth edition, 2016.

[15] P. Coleman.
Introduction to Many-Body Physics.
Cambridge University Press, 2015.

[16] G. D. Mahan.
Many-Particle Physics.
Springer Science & Business Media, 2000.

Influence of magnetocaloric and electrocaloric effects on spin conductivity of an open Fermi-Hubbard lattice

Vladimir P. Villegas [1]

10 November 2023

[1]Department of Mathematics and Physics,
College of Science, University of Santo Tomas,
España Blvd., Sampaloc 1008 Manila